32nd URSI GASS, Montreal, 19–26 August 2017

Antenna Measurements through Planar Near Field Apparatus: An Educational Paradigm Linking Electromagnetic Theory, Sampling Techniques, and FFT

Yahya Rahmat-Samii and Joshua M. Kovitz
(1) Electrical Engineering Department, University of California Los Angeles
Los Angeles, CA, USA http://www.antlab.ee.ucla.edu

Abstract

Integrating antenna pattern measurements in the classroom offers many captivating insights about electromagnetic fields that is visually appealing to young scientists and students. In particular, the planar near-field measurement techniques allow instructors to connect to fundamental knowledge about antennas. Challenging concepts become immediately a hands-on discussion while providing students an important application of fundamental electrical engineering and electromagnetic theories. Our tabletop bipolar apparatus also brings out a discussion on the challenges of measurements at high frequencies, such as mmWaves, where cable movement and flexing can cause significant errors. This paper suggests planar near-field measurements as an educational paradigm linking electromagnetic theory, sampling techniques, and FFT.

1 Introduction

Antenna pattern measurements is an exciting area to aid with student teaching and inspiration. Among various antena pattern measurement techniques, near-field measurements have everything that an instructor would hope to include in a stimulating educational experience. A complete experience with near-fields would engage students with deep electromagnetic theories, tradeoff studies, engineering practice, design principles, and a little glamour from the robotics, laser positioning metrology, and visually appealing absorber. Among the three spherical, cylindrical, and planar near-field techniques, the class of planar techniques make for a complete and easy-to-access discussion in a lecture. The advantage is that planar near-field techniques can employ the Fast Fourier Transform (FFT) based on the Fourier transform relationship between planar near-fields and antenna far-fields. The Fourier transform is often more accessible for undergraduate and graduate students to visualize, and even students interested in signal processing can get a strong feeling about electromagnetic fields.

In this paper, our hope is to encourage readers, instructors (future and current), and mentors that planar near-field measurements can provide a holistic educational experience for students. We will focus on our bipolar near-field chamber that was developed as a tabletop anechoic chamber for mmWave measurements at UCLA [1, 2], but these experiences can be easily applicable for plane-polar and plane-rectangular chambers as well. By integrating this material into regular classroom lectures, potentially more students can get excited about antenna radiation metrology, which involves expertise beyond electromagnetics. We also provide an example where we show the step-by-step implementation being executed for a measurement.

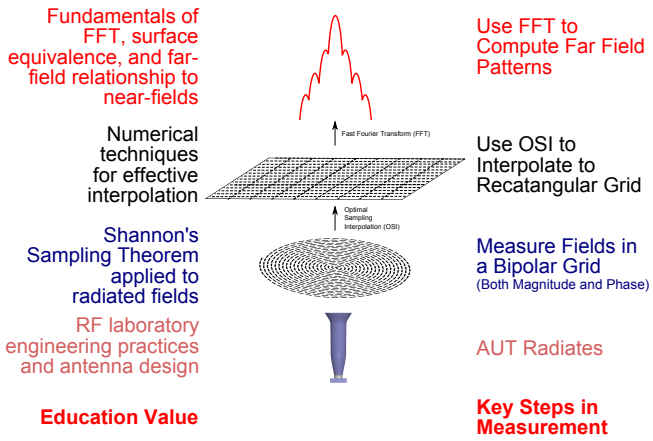

Figure 1. Illustration of the steps used to measure an antenna far-field pattern with a planar bipolar near-field chamber. The corresponding educational component for each key step in the measurement process is also illustrated.

2 Relating Pattern Measurements to the Fundamentals

Antenna metrology is an interesting area because it involves fundamentals from many areas within electrical engineering. Figure 1 highlights the educational component that each step within an antenna near-field measurement provides in the context of a bipolar chamber [1, 2]. In this section we walk step-by-step through each major educational component and discuss how instructors can relate the measurement experience with an application of electrical engineering and electromagnetics fundamentals.

2.1 AUT Positioning and Good Lab Practice

The first step in conducting a near-field measurement is the physical set up. This is possibly the most important and challenging step within the entire measurement process.

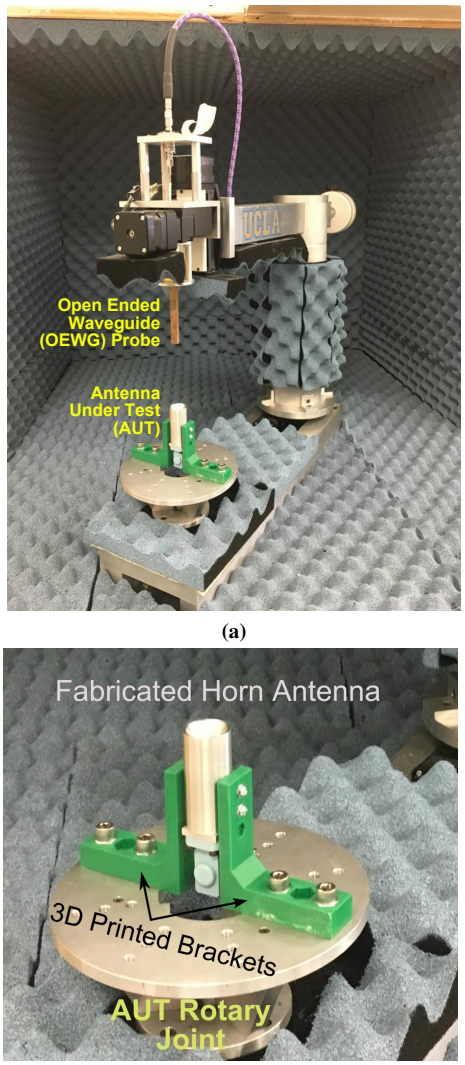

(a)

(b)

Figure 2. (a) Tabletop bipolar anechoic chamber to help students visualize and understand radiated electromagnetic fields from a variety of antennas like horns, arrays, etc. (b) Magnified view of an example antenna under test (AUT), which is a spline-profiled horn antenna from [3].

Poor alignment and positioning errors can lead to noticeable phase errors in the near-field, resulting in dramatic errors in the far-field. This step provides an opportunity for instructors to discuss the operation of robotics equipment and stepper motors. It also provides an opportunity for students to get creative when developing brackets and positioning equipment. For our particular example in Figure 2, the students opted to 3D print the bracket. While plastic 3D printing methods do not provide the best resolution, it made for a nice educational moment where students satisfied their curiosity in fabricating important engineering designs using 3D printers.

Another learning component in this step is the proper usage of sensitive RF equipment. At this point, instructors can incorporate good RF engineering practices into the lab discussion, where proper handling of coaxial cable, connectors, antenna probes, and connector mating can be strongly emphasized. Students also get a chance to learn how to use valuable equipment such as spectral analyzers, RF power meters, and vector network analyzers (VNA's). In near-field

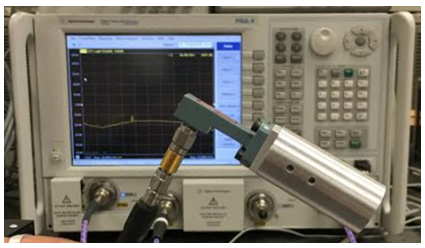

Figure 3. Near-field chambers require both magnitude and phase values, necessitating the use of high-performance VNA measurements.

measurements, VNA's are employed because both magnitude and phase information is needed to perform the near-field to far-field transformations in post-processing. Our tabletop bipolar anechoic chamber is connected to an Agilent PNA-X 5247A, as shown in Fig. 3, which can measure well into the mmWave bands with this configuration.

2.2 Shannon's Theorem and Radiated Fields

With the physical measurement setup complete, the next important question is in the sampling locations for the electric fields. The bipolar configuration uses two rotational stages to position the probe. In Figure 4, we illustrate the sampling locations with respect to the bipolar coordinates (β, α), where the AUT rotation determines α and the bipolar arm rotation determines β [1, 2].

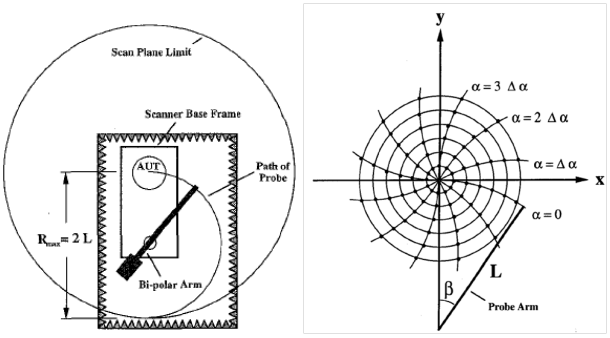

(a) (b)

Figure 4. (a) The bipolar measurement configuration uses two rotational stages to position the probe, where α is controlled by rotating the AUT, β is controlled by rotating the bipolar arm. (b) Illustration of the bipolar coordinates β and α. The sample intervals $\Delta\beta$ and $\Delta\alpha$ are important to determine for proper sampling. Figures adapted from [1].

Ultimately, we are sampling the electric field (magnitude and phase) in discrete points in space, with the hope to ascertain all pertinent information about those fields. Shannon's theorem tells us that perfect reconstruction from a

sampled function can only occur when the original function is bandlimited. In this respect, there are two important considerations to be understood. First, the far-field radiation patterns are computed from a Fourier Transform of the near-field data, allowing the use of the FFT operation. Using currently available, efficient FFT techniques means that we must provide the data in a rectilinear grid. Assuming that no evanescent spectral components exist in the measurement plane (this is a good assumption if we are in the radiating near-field zone of the antenna), then the maximum spatial variation observed in the near-field is k_0, the free-space wave number. Analgous to signal processing, this means that our sampling spacing for this rectilinear grid must be [4]

$$\Delta x, \Delta y \leq \frac{\pi}{k_0} = \frac{\lambda_0}{2} \tag{1}$$

where λ_0 is the free-space wavelength. This is analogous to the time sample intervals $\Delta t = 1/2f_{\max} = \pi/\omega_{\max}$, where $f_{\max}$ and $\omega_{\max}$ are the maximum frequency and angular frequency components of the time-varying signal.

The second important consideration is that the bipolar grid data must be interpolated to a rectilinear grid. In the early days of planar near-field measurements, the general consensus was to choose sample spacings such that the arc between adjacent points was roughly $\lambda_0/2$ [5]. However, studies in [6] revealed that the near-field distributions could be even more bandlimited if the proper mathematical modification to the fields could be made. These potential modifications to the fields (spherical phase cancellations) are discussed in the next section. These studies ultimately determine the sampling intervals $\Delta\beta$, $\Delta\alpha$, with respect to the bipolar coordinate system, that ensures the proper intervals [1, 2]. This proper spacing allows us to interpolate the data onto a rectilinear grid with intervals $\lambda_0/2$ or less.

2.3 Interpolation

Once the fields have been sampled in their respective grid, the fields must be interpolated into a rectilinear grid. We do the interpolation so that we can apply the FFT operation onto the near-field data. The very large amount of interpolant data makes the interpolation very cumbersome and time-consuming. As previously mentioned, studies have shown that the radiated fields from a given AUT could

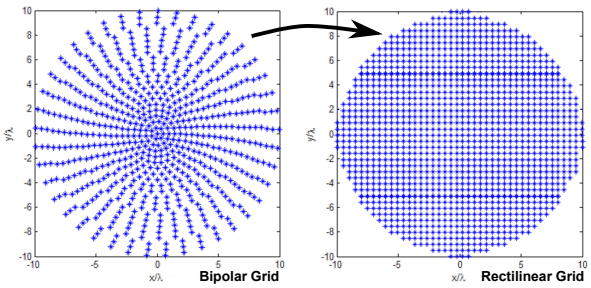

Figure 5. Interpolation from a bipolar grid to a rectilinear grid. Note that values outside the circle are set to zero.

be made bandlimited by cancelling the spherical phase $\exp(-jkr)$. This removes the rapid oscillations of the near-fields observed from the $\exp(-jkr)$ factor. After removing these oscillations, an interpolation called Optimal Sampling Interpolation (OSI) can be employed, which interpolates along β with the $\mathrm{sinc}(\cdot)$ function and along α with the Dirichlet function [6, 7]. The interpolation between the bipolar grid and rectilinear grid is illustrated in Figure 5.

2.4 Surface Equivalence

The surface equivalence theorem provides the theoretical basis for all of near-field measurements, and it is often a challenging theorem to grasp without the help of measurements [1]. Fundamentally, the surface equivalence theorem states that we can enclose a radiator with a fictitious surface and create equivalent electric and magnetic currents that are impressed tangentially along this surface outside the volume. By "equivalent", we mean that the radiation from these equivalent currents will be identical to the original radiator inside the surface. This is illustrated in Figure 6,

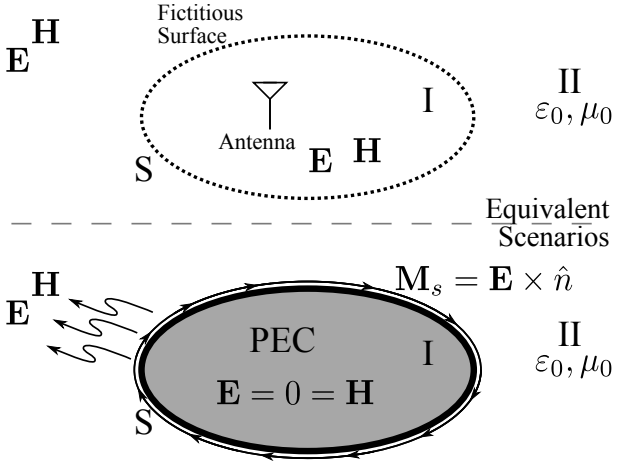

Figure 6. Illustration of Love's equivalence theorem, which justifies near-field measurements using Maxwell's equations [1]. Introducing PEC allows the usage of the equivalent magnetic current, simplifying the measurement by only using an electric field probe (OEWG in Fig. 2).

where a radiator was enclosed by a fictitious surface and replaced by an equivalent magnetic surface current $\mathbf{M}_s$. The major breakthrough from this principle is that knowledge of the radiated fields is completely known when we sample the tangential fields on a closed surface around the antenna, even in the near-field. Furthermore, we only have to sample the electric field, which can be used to create the fictitious magnetic surface current $\mathbf{M}_s$. This is one of the exciting links between near-field measurements and electromagnetic theory, and it very clearly demonstrates the importance of understanding these fundamental theorems.

3 Fourier Transforms and the FFT

At this point, we have the data on a plane (ideally extended to infinity), which effectively creates a closed surface around the AUT. After the OSI interpolation, we would

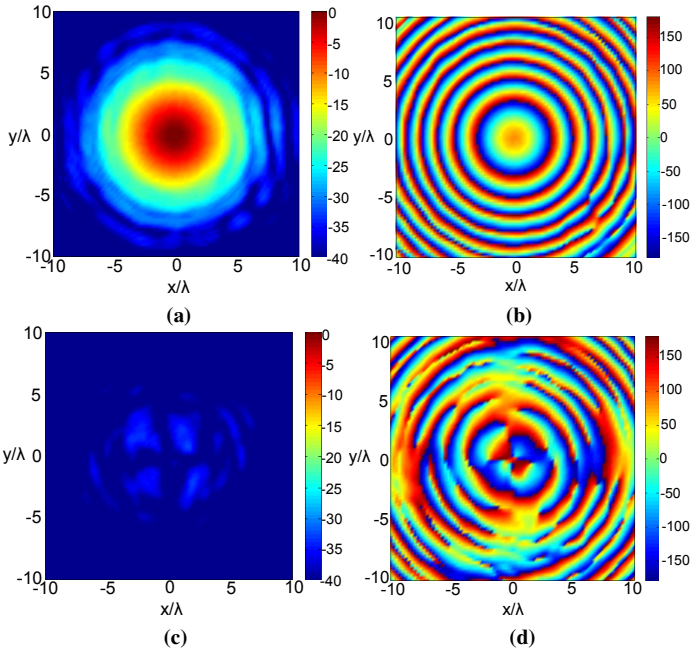

Figure 7. Measured near field aperture distributions after OSI interpolation at 35.75 GHz (a) Copol amplitude distribution, (b) Copol phase distribution. (c) Xpol amplitude distribution. (d) Xpol phase distribution.

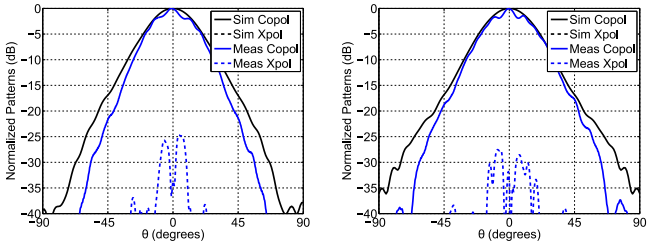

Figure 8. Resulting far field pattern for the AUT at 35.75 GHz. These patterns were generated using the FFT operation. (a) E-plane pattern. (b) H-plane pattern.

have data that appears as shown in Figure 7, which are the so-called near-field plots of the magnitude/phase values for E_x and E_y. This near-field data can then be used to obtain the far-field patterns of the AUT. Since the near-fields are on a plane, the far-fields share a Fourier transform relationship with the near-fields. This is a direct result of the vector potential integration of the equivalent magnetic surface current $\mathbf{M}_s$ by

$$\mathbf{E}_{ff}(k_x,k_y) \propto \iint_{-\infty}^{\infty} \mathbf{E}_{nf}(x,y,0) \times \hat{n} e^{jk_x x' + jk_y y'} dx'dy' \quad (2)$$

where $\mathbf{E}_{ff}$ is the far-field electric field, $\mathbf{E}_{nf}$ is the near-field electric field, and $\hat{n}$ is the normal to the measurement plane. Note that this integral is often truncated when the near-field levels drop below a given threshold, usually below -40 dB. The final far-field patterns are shown in Figure 8, where a nice beam radiating from the horn antenna is measured. Clearly other steps such as probe pattern compensation are also required to get highly accurate far field pattern at wide angles [1]. Instructors can use several examples of different AUT measurements to illustrate this 2D Fourier relationship between the near-fields and far-fields.

4 Concluding Remarks and Discussion

In our experience, the planar near-field antenna measurement techniques makes a nice, complete example for students to grapple with electromagnetic and electrical engineering principles. Our tabletop bipolar near-field apparatus represents the embodiment and application of many fundamental electrical engineering and electromagnetic principles. This hands-on approach with teaching is invaluable to students, where students can better visualize fields, sampling techniques, and electromagnetic theory. At the same time, students are also exposed to the fun world of antenna metrology, where engineers can readily get hands-on experience in a number of related fields such as robotics, programming, and laser positioning systems. There are ample, relevant references in [1] for further reading and details.

5 Acknowledgements

The authors would like to thank Vignesh Manohar for helpful discussions.

References

[1] Y. Rahmat-Samii, L. Williams, and R. Yaccarino, "The ucla bi-polar planar-near-field antenna-measurement and diagnostics range," *IEEE Anten. Prop. Mag.*, **37**, 6, pp. 16–35, 1995.

[2] T. Brockett and Y. Rahmat-Samii, "A novel portable bipolar near-field system for millimeter-wave antennas: construction, development, and verification," *IEEE Anten. Prop. Mag.*, **50**, 5, pp. 121–130, 2008.

[3] J. Kovitz, V. Manohar, and Y. Rahmat-Samii, "A spline-profiled horn antenna assembly optimized for deployable Ka-band offset reflectors in CubeSats," in *IEEE Int. Symp. Anten. Prop.*, 2016, pp. 1535–36.

[4] J. M. Kovitz and Y. Rahmat-Samii, "Novelties of spectral domain analysis in antenna characterizations: Concept, formulation, and applications," in *Advanced Computational Electromagnetic Methods*, W. Yu, W. Li, A. Elsherbeni, and Y. Rahmat-Samii, Eds. Artech House Publishers, 2015, ch. 1, pp. 1–82.

[5] M. Gatti and Y. Rahmat-Samii, "FFT applications to plane-polar near-field antenna measurements," *IEEE Trans. Anten. Prop.*, **36**, 6, pp. 781–791, 1988.

[6] O. M. Bucci, C. Gennarelli, and C. Savarese, "Fast and accurate near-field-far-field transformation by sampling interpolation of plane-polar measurements," *IEEE Trans. Anten. Prop.*, **39**, 1, pp. 48–55, 1991.

[7] S. Razavi and Y. Rahmat-Samii, "A new look at phaseless planar near-field measurements: limitations, simulations, measurements, and a hybrid solution," *IEEE Anten. Prop. Mag.*, **49**, 2, pp. 170–178, 2007.